

# Measurements of the Collection Efficiency of an Air Cyclone in Lunar Gravity

Kevin M Crosby<sup>1</sup>, Juan Agui<sup>2</sup>, Caitlin Pennington<sup>1</sup>, Emily Sorensen<sup>3</sup>,  
Erin Martin<sup>1</sup>, Isa Fritz<sup>1</sup>, and Brad Frye<sup>1</sup>

<sup>1</sup>Department of Physics, Carthage College, Kenosha, WI

<sup>2</sup>NASA Glenn Research Center, Cleveland OH

<sup>3</sup>College of Engineering, University of Wisconsin, Madison, WI

## Abstract

We report experimental results on the collection efficiency of an air cyclone operating with a lunar dust simulant under lunar gravity. Microgravity collection efficiency is, to within experimental uncertainty, not different from collection efficiencies obtained in one-g experiments. We discuss a heuristic model of particle motion in an air cyclone that accounts for this unexpected result, and provide a framework for future experiments to clarify the operational properties of cyclone filtration systems in microgravity.

## 1 Introduction

Air cyclones are used throughout industry in diverse filtration applications including particle segregation and separation in the pharmaceutical industry, dust mitigation in factory settings, and in ambient air sampling applications. The simple design of a typical cyclone separator involves no moving parts or replaceable filtration media. Cyclone separators are therefore robust against failure and have significantly lower operating costs than alternative filtration strategies. For these reasons, cyclone-based particle collection may be viable as a first-stage filtration technology in future lunar habitats where dust mitigation is a central concern.

While a variety of cyclone designs and operating parameters have been explored in the literature, cyclone operating properties are understood primarily through empirical or semi-empirical models [Boysan *et al.*, 1982]. The complex fluid dynamics of air flow in the constrained geometry of the cyclone prohibits a fundamental analysis of cyclone efficiency. Such analysis would presumably elucidate the role of gravitational settling in the efficiency measures of an air cyclone. However, the role of gravity in the operation of an air cyclone had not been studied experimentally. In this

paper, we report on cyclone experiments with the lunar dust simulant conducted in the microgravity environment of the NASA *Weightless Wonder* aircraft [NASA].

Our experiment team consists of five undergraduate researchers (Fritz, Frye, Martin, Pennington, and Sorensen), a NASA mentor (Agui), and a faculty advisor (Crosby) who all had the opportunity to participate in the inaugural NASA *Systems Engineering Education Discovery* (SEED) program. The SEED program offers undergraduate teams the opportunity to design, build, and fly a microgravity experiment to support the research initiatives of the NASA sponsor.

## 2 Properties of Lunar Dust

The lunar regolith is a layer of unconsolidated material covering the lunar surface to depths of several meters. The regolith material is formed through micrometeorite impacts on the surface of the moon. While the composition of the regolith varies across the lunar surface, the primary constituent of the regolith near the surface of the moon is a fine powdery dust of metallic oxides and silicates. The distribution of particle sizes in the dust is quite broad, ranging from submicron particles to particles in the 100+ micron range [Park *et al.*, 2006]. Of particular concern for long-term human presence on the moon, is the fine portion of the size distribution, those particles with diameters less than  $50 \mu\text{m}$ . By number these particles represent nearly 50% of lunar dust samples returned from Apollo missions.

This dust has been identified as a significant hazard to future lunar missions due to its presumed human toxicity [Park *et al.*, 2006]. In the vernacular of physiological effects associated with particulate pollution, approximately 5% of lunar dust by volume is *respirable*, having aerodynamic diameters of less than  $4 \mu\text{m}$ .

The adverse health effects of airborne lunar dust on Apollo astronauts have been well-documented [Park *et al.*, 2006]. The effect of lunar dust on mission critical technologies has also been documented [Gaier, 2008]. The pervasive presence of regolith dust on the moon poses technological challenges to a sustained human presence on the moon. Mitigation of lunar dust in planned lunar base facilities is a high priority technology goal in the NASA Return to the Moon program. In our experiments, we use the lunar dust simulant JSC -1AF, a basaltic ash powder that reproduces the grain size distribution and some of the morphological attributes of the fine regolith dust in the lunar *mare* regions [Orbitec, Inc.].

## 3 Cyclone Operating Principles

An air cyclone is a device that separates particles from a carrier air stream by means of a centrifugal force acting on the particles. The essential geometry of an air cyclone is depicted in Fig. 1. Dust particles, initially entrained in the air flow, enter the tangential inlet near the top of the cyclone, and follow the downward spiral of the air vortex. Centrifugal force and inertial effects act on the

particles to move them outward toward the inner wall of the cyclone where they are trapped in the boundary flow. Trapped particles eventually move down the inner wall and are collected in a dust cup at the base of the cyclone while the air flow reverses direction near the base of the cyclone, and exits the through the vortex finder at the top of the cyclone.

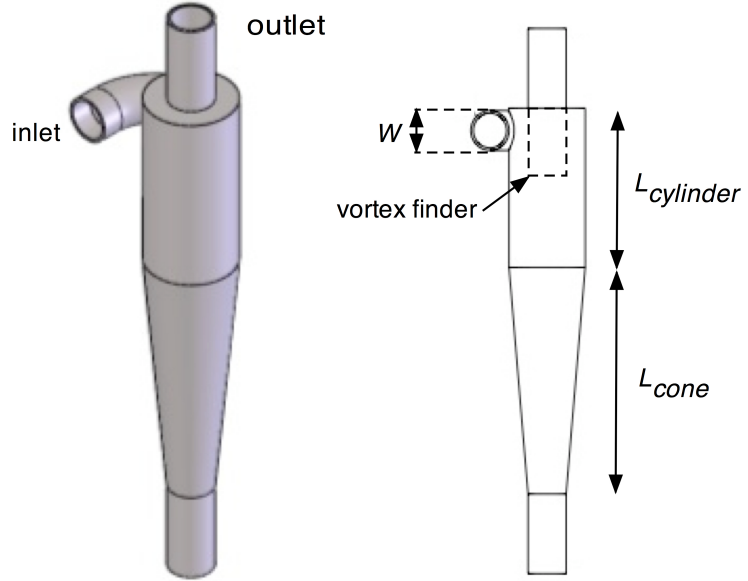


Figure 1: The geometry of the air cyclone used in this study. The cyclone consists of a straight cylinder with diameter 5.08 cm and length  $L_{cylinder} = 10.5$  cm, a cone of length  $L_{cone} = 14.0$  cm, and a cylindrical vortex finder of diameter 2.54 cm. Dust-laden air is introduced through the inlet of diameter  $W = 2.54$  cm. A dust cup is attached to the bottom of the cyclone.

## 4 Experimental Rig

A schematic of the flight rig used in this study is shown in Fig. 2. An oilless regenerative blower is used to pull ambient air through the system. Ambient air is initially pulled through F1 which is an 0.01  $\mu\text{m}$  HEPA compressed air filter rated at 64 cfm.  $F_1$  removes any particulate matter in the airstream, ensuring that the lunar dust simulant is the only significant source of particulates in the system. The dust is introduced into the airstream by the fluidizing tank. The tank is a PVC cylinder 4" in diameter and 18" high. Approximately 200 grams of JSC-1AF simulant is loaded in the cup at the bottom of the tank, and air is introduced through the inlet arm which is at a 45° angle from the axis of the tank. The dust is fluidized in the tank and exits with the airstream at the top of the tank where it is mixed with clean air. The concentration of simulant in the system can be controlled with the valve  $V_1$  which bleeds in clean air.

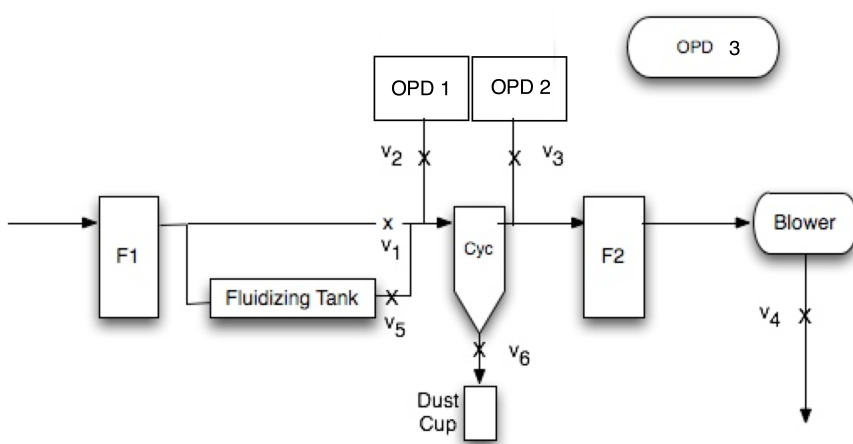


Figure 2: Air flow through the cyclone is driven by the blower and controlled by valve  $V_4$ . Ambient air is pulled through the HEPA filter  $F_1$  and mixed with lunar dust simulant in the fluidizing tank. Dust counts are recorded both pre- and post-cyclone by optical particle detectors  $OPD_1$  and  $OPD_2$ . HEPA filter  $F_2$  is used to remove the residual dust before the air is exhausted to the environment.

The airstream enters the cyclone through the tangential inlet and exits through the axial finder tube along the central axis of the cyclone. Trapped dust enters the cup at the bottom of the cyclone. The airstream downstream of the cyclone undergoes a final filtration stage to remove the smaller particles not trapped by the cyclone. Final filtration is accomplished by  $F_2$  which is identical to  $F_1$ .

To maintain a sufficient flow rate and to minimize frictional losses, our components are connected by 1" I.D. tubing. A consistent electrical ground is maintained across all components and throughout the flow circuit by utilizing anti-static (conductive) tubing. This is necessary to ensure accurate particle counts by eliminating electrostatic interactions between simulant particles and component and tube interiors. All components have conducting interiors that are electrically connected to a common ground. Flow rate is controlled by valve  $V_4$ , and can be varied between 0 and 18 cfm.

#### 4.1 Instrumentation

Two optical particle detectors were used to monitor dust counts, one was positioned just before the cyclone to record pre-cyclone particle counts, while the second was positioned at the cyclone outlet to record post-cyclone particle counts. Both particle detectors were Lighthouse Handheld 3016 IAQ laser particle detectors with 1/2-inch isokinetic sampling probes and internal sampling pumps [Lighthouse, Inc.]. A third particle detector, an AM510 personal aerosol monitor, was used to monitor ambient air for possible dust contamination. The Lighthouse detectors can record particle counts in six simultaneous channels. Each channel is calibrated for a specific range of aerodynamic particle diameters. To optimize counts relative to the grain size distribution of the

JSC-1A simulant, our particle channels were set to the diameter ranges  $d_p$ : ( $0.3 \leq d_1 < 0.5$ ,  $0.5 \leq d_2 < 1.0$ ,  $1.0 \leq d_3 < 3.0$ ,  $3.0 \leq d_4 < 5.0$ ,  $5.0 \leq d_5 < 10.0$ ,  $d_6 \geq 10$ )  $\mu\text{m}$ .

The optical particle detectors  $\text{OPD}_1$  and  $\text{OPD}_2$  each have internal pumps to draw air from the flow lines to the detector units. The sampling lines passing through valves  $V_2$  and  $V_3$  in Fig. 2 are 1/2-inch I.D. silicone tubes that connect to the flow lines by Y-shaped hose connectors that maximize the degree of isokinetic flow sampling to the extent possible. At a flow rate of  $Q = 10$  cfm, flow through the cyclone suffers a pressure drop of  $2 \times 10^3$  Pa. This pressure drop causes flow speeds to differ at the pre- and post-cyclone sampling locations. As a result, the two particle detectors  $\text{OPD}_1$  and  $\text{OPD}_2$  experience different back-pressures with  $\text{OPD}_1$  fighting a larger suction than  $\text{OPD}_2$  as its internal pump attempts to draw air for sampling. We compensate for this effect by normalizing particle counts obtained by  $\text{OPD}_1$  and  $\text{OPD}_2$  by the volume of air sampled by each detector per unit time.

Finally, using a Kestrel 3500 Wind Meter, flow rates were monitored at the air inlet to ensure consistent flow during the data collection. Valve  $V_4$  was used to adjust flow to compensate for reduced cabin pressure at altitude. Flow through the cyclone was fixed at 10 cfm for all data runs reported here.

## 4.2 Cyclone

The cyclone used in our experiments is a steel unit with dimensions noted in Fig. 1. The cyclone separator accepts dusty air through an inlet on the side, and due to the conical shape of the cyclone body, induces the air to move tangentially to the inner surface of the cyclone. The air orbits in a helix of decreasing diameter as it travels down the axis of the cyclone. Heavier particulate matter is centrifugally trapped by the walls of the cyclone where it leaves the air stream and either sticks to the wall or migrates to a collection cup at the bottom of the cyclone. The rotating air is exhausted through an axial outlet at the top of the cyclone where it can be processed further with traditional filter media to remove the remaining particulate matter.

Several semi-empirical models of cyclone efficiency calibrated for specific cyclone geometries are available in the literature [Iozia *et al.*, 1989]. The principal measures of cyclone performance models are the fractional collection efficiencies  $\epsilon_i$  for particles with diameters  $d_i$ , the cut-size  $d_{50}$  which represents the minimum diameter at which the cyclone can be expected to filter at least 50% of the particles, and the pressure drop  $\Delta P_{\text{cyclone}}$  across the cyclone. Both  $d_{50}$  and  $\Delta P_{\text{cyclone}}$  depend on the flow-rate  $Q = v_{\text{in}} A$  through the cyclone where  $v_{\text{in}}$  is the gas velocity at the inlet of cross-sectional area  $A$ .

We will adopt the Lapple model [Shepherd *et al.*, 1940], which defines the fractional collection efficiency for particles of aerodynamic diameter  $d_i$  as

$$\epsilon_i = \frac{1}{1 + (d_{50}/d_i)^2}. \quad (1)$$

The expression for  $d_{50}$  in the Lapple model is a function of the geometric properties of the cyclone,

and the kinematic properties of the gas. The former are defined in Fig 1. The semi-empirical result for  $d_{50}$  in the Lapple model is

$$d_{50} = \left[ \frac{9\eta W^2}{\pi v_{in}(2L_{cylinder} + L_{cone})(\rho_p - \rho_g)} \right]^{1/2}, \quad (2)$$

where  $\eta = 1.75 \times 10^{-5}$  Pa-sec. is the dry-air viscosity, and  $\rho_p = 2900$  kg/m<sup>3</sup> and  $\rho_g = 1.3$  kg/m<sup>3</sup> are the mass densities of the particles and gas, respectively.

At a flow rate of  $Q = 10$  cfm, Eqn. 2 predicts a cut-size of  $d_{50} = 1.8\mu\text{m}$ . According to Eqn. 2, we expect  $d_{50} \propto Q^{-1/2}$  so that by varying flow-rates between 10 and 18 cfm, the cyclone can be tuned to achieve values of  $d_{50}$  in the range of  $1.8\mu\text{m}$  to  $1.3\mu\text{m}$ .

## 5 Flight Data

The *Weightless Wonder* is a modified C-9 aircraft used in the parabolic flight program operated by NASA's Reduced Gravity Office [NASA]. The trajectory of the parabolic dive can be modified to provide periods of microgravity from zero-g through hyper-gravity ( $g > 9.8$  m/s<sup>2</sup>). Our experiment took place over two flights each consisting of 30 parabolas, 20 of which provided lunar gravity (1/6 of the gravitational acceleration on the surface of the earth). Each parabola generated approximately 30 seconds of lunar gravity in which to make collection counts, for a total of approximately 20 minutes of total flight time in lunar gravity, yielding approximately  $10^7$  particle counts.

During the flights, the blower operated continuously to maintain a relatively constant, low-density dust fraction in the air flow for all data runs. The particle detectors were calibrated and cross-checked for consistency prior to each flight and were programmed to only take data during the microgravity portions of the parabolas. The size distribution of dust simulant as measured by the pre-cyclone particle detector remained constant throughout the data acquisition period, and is shown in Fig. 3.

Collection efficiencies for each particle size  $i$  were computed according to

$$e_i = \frac{N_i - N'_i}{N_i} \quad (3)$$

where  $N_i$  is the number of particles with diameter  $d_i$  per unit time recorded by the pre-cyclone detector, and  $N'_i$  is the number of particles with diameter  $d_i$  per unit time recorded by the post-cyclone detector.

Collection efficiencies were computed for each 30-second parabola. The individual efficiencies were averaged and standard errors computed over the set of parabolas for each diameter range. These results are displayed in Fig. 4. Data for one-g collection measurements are also shown in

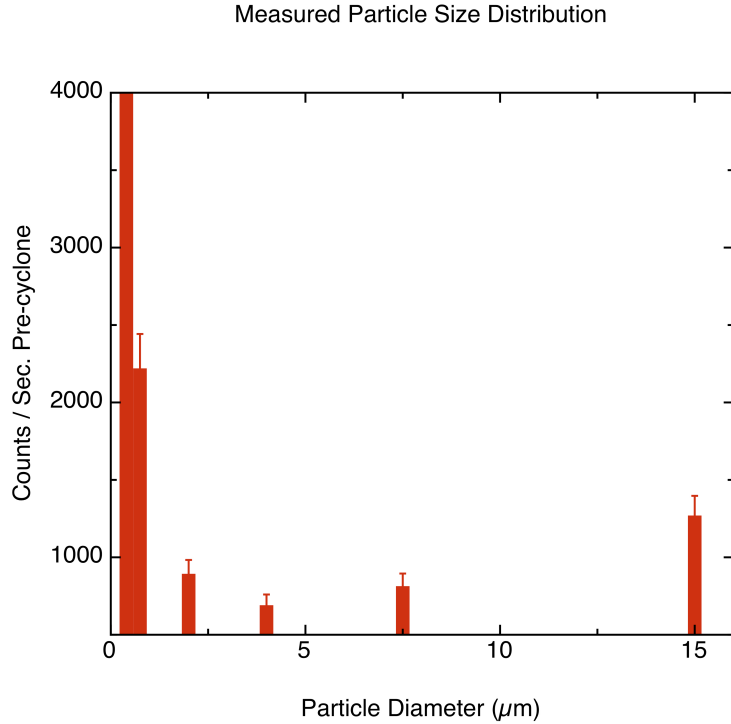


Figure 3: Particle size distribution in the dust simulant. Vertical error bars represent standard errors for thirty 30-second measurements. Horizontal errors are not indicated, but data bars are positioned at the midpoints of each particle channel.

Fig. 4. Our one-g data was taken under the same flow conditions as the flight data. Also shown in Fig. 4 is a plot of the Lapple model fit for a cyclone with  $d_{50} = 1.8\mu\text{m}$  corresponding to the anticipated cut-size for our 10 cfm flow rate. As expected the Lapple model data underestimates the efficiency of our cyclone. The reason is that the Lapple model describes a standard Stairmand cyclone that has different geometrical properties than the modern, high efficiency cyclones or “sharp-cut” cyclones available today [Stairmand, 1951].

## 6 Analysis

It is clear from Fig. 4 that reduced gravity collection efficiencies do not differ significantly from those obtained in earth gravity. This is a somewhat unanticipated result given the premise that collection occurs in part by gravitational settling of dust down to the dust cup at the base of the cyclone. We might expect a moderate reduction of collection efficiencies in reduced gravity due to the longer migration time for particles to reach the dust cup. Instead, to within statistical uncertainty, we find no difference in collection efficiency between the two different gravitational fields considered here.

These results can be understood in terms of a simple model of particle motion in the cyclone

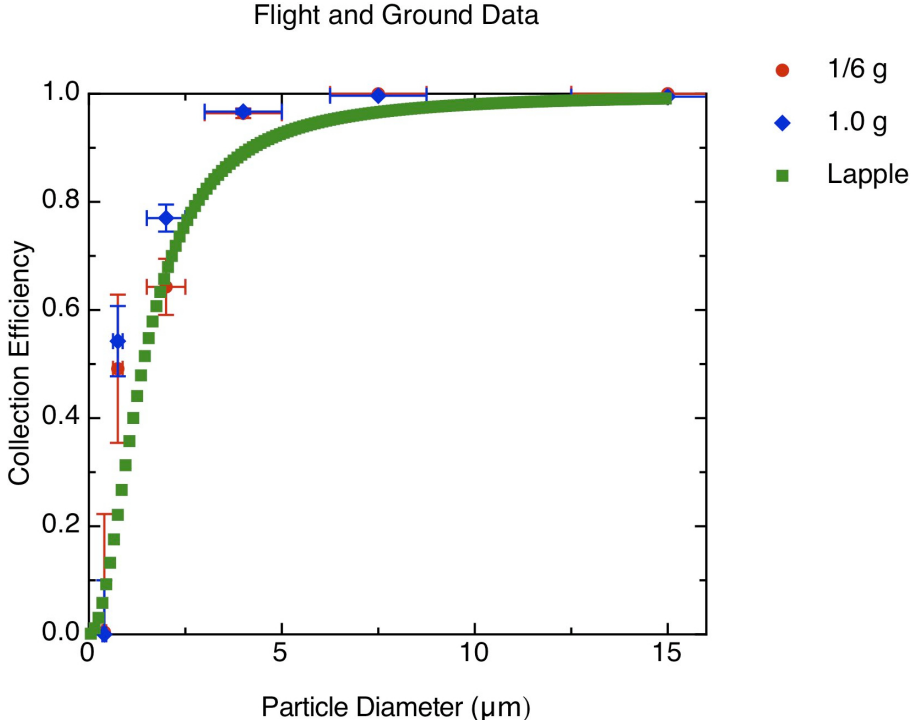


Figure 4: Experimental results ( $\bullet$  and  $\diamond$ ) and Lapple Model predictions ( $\blacksquare$ ) for the performance of the model cyclone used in this study. The width of the error bars on the experimental data represents the uncertainty in particle size measurements in the particle detector used. The heights of the error bars on the experimental data are the standard deviations of the collection efficiency measurements. The Lapple model data is a fit of the cyclone performance predictions derived from the work in Ref. [Shepherd *et al.*, 1940].

separator. This analysis is carried out in a companion paper on modeling particle collection through computational fluid dynamics, and the reader is referred there for details [Crosby *et al.*, 2008]. The important results of the model in Ref. [Crosby *et al.*, 2008] is that the radial motion of a particle subject to centrifugal, drag, and buoyant forces in the radial direction is entirely dependent on kinematic properties of the flow and geometrical properties of the cyclone. The radial motion of particles in a cyclone does not depend on gravity. Outward migration of particles from an initial position in the cyclone to entrainment in the boundary flow at the wall of the cyclone occurs over time scales that do not depend on the value of  $g$ . Our CFD calculations suggest that the boundary flow near the inner wall of the cyclone ultimately results in the particle being trapped on the wall or migrating down the wall toward the dust cup even in the absence of gravity. The CFD calculations and the analytical model of particle motion in cyclone separators described in Ref. [Crosby *et al.*, 2008] reconcile our experimental results for collection efficiencies under earth and lunar gravity. In particular, our analytical model of particle motion suggests that the time required for a particle to migrate from an initial radial position  $R_0$  to a final radial position  $R$  called the

*residence* time, and is given by

$$\tau_{\text{residence}} = \frac{18\eta}{(\rho_p - \rho_g)\omega^2 d_p^2} \log\left(\frac{R}{R_0}\right). \quad (4)$$

Note that Eqn. 4 is independent of gravity, and that the residence time appears to be function of the cyclone geometry, kinematic properties of air, and the particle diameter.

Axial motion of particles in air cyclones is governed by drag, buoyancy, and gravitational forces. Axial accelerations are brief, and the axial component of motion in the context of the simple model in Ref. [Crosby *et al.*, 2008] is described by a terminal velocity component

$$v_{zT} \equiv \dot{z}|_{\text{terminal}} = -\frac{(\rho_p - \rho_g)d_p^2}{18\eta}g \quad (5)$$

which is on the order of  $10^{-4}$  m/s for  $1 \mu\text{m}$  particles. Here,  $z$  is the axial coordinate increasing up from the base of the cyclone, and  $d_p$  is the particle's aerodynamic diameter. For the range of particle diameters considered in this study, axial terminal speeds are negligibly small under both lunar and earth gravity. Gravitational influences on particle capture are therefore negligible for the relatively small cyclone that we used. The efficiency of larger cyclones may indeed exhibit more pronounced gravitational dependence due to gravity-driven turbulence instabilities in large-scale flow. Experimental and computational investigations of larger cyclones in microgravity need to be carried out in order to take further steps toward validating inertial filtration technologies in reduced gravity environments.

## 7 Summary and Discussion

We have measured the fractional collection efficiency of a model cyclone separator in both lunar and earth gravity with a lunar dust simulant. Within the resolution of our experiment, we find no meaningful difference in the overall collection efficiencies measured under the different gravitational conditions. This result suggest that air cyclones may be a viable first stage filtration technology for removal of airborne lunar dust from human environments on the moon. Given commercial interest in mining and processing of the moon's rich mineral and chemical landscape, the viability of air cyclones for particle segregation and separation may also provide a promising avenue for future research in *in situ* lunar resource utilization.

## 8 Acknowledgments

The authors gratefully acknowledge the Wisconsin Space Grant Consortium and the Carthage College Student Government for financial support.

## References

- [Boysan *et al.*, 1982] See for instance, Boysan, F., Ayers, W.H., and Swithenbank, J., A fundamental mathematical modeling approach to cyclone design, *Trans Inst Chem Eng*, **60** (1982).
- [Crosby *et al.*, 2008] Crosby, K. M. and Frye, B., Computational Fluid Dynamical Model of a Cyclone Separator in Microgravity, *2008 Proceedings of the Wisconsin Space Grant Consortium* (2008).
- [Gaier, 2008] Gaier, J. R., The Effects of Lunar Dust on EVA Systems During the Apollo Missions, *NASA Technical Report* <http://gltrs.grc.nasa.gov>. Retrieved April 16, 2008.
- [Iozia *et al.*, 1989] See for example, Iozia, D. L. and Leith, D., Effect of Cyclone Dimensions on Gas Flow Pattern and Collection Efficiency, *Aerosol Science and Technology*, **10** 491 (1989).
- [Lighthouse, Inc.] Lighthouse Worldwide Solutions, Fremont, CA.
- [NASA] NASA Reduced Gravity Office, Johnson Space Center, Houston, TX.
- [Orbitec, Inc.] JSC-1AF lunar regolith dust simulant manufactured by Orbitec, Inc. and provided by Juan Agui, NASA Glenn Research Center.
- [Park *et al.*, 2006] Park, J.S.; Y. Liu, K. D. Kihm, and L. A. Taylor, Micro-Morphology And Toxicological Effects Of Lunar Dust, *Lunar and Planetary Science XXXVII* (2006).
- [Shepherd *et al.*, 1940] Shepherd, C. B., and Lapple, C. E., Flow Pattern and Pressure Drop in Cyclone Dust Collectors, *Industrial and Engineering Chemistry* **32**, 1246 (1940).
- [Stairmand, 1951] Stairmand, C. J., The Design and Performance of Cyclone Separators, *Trans. Instn. Chem. Engrs.* **29** (1951).